Gold Nanostar@Prussian Blue Core-Shell Nanoparticles for the Detection of Acute Myocardial Infarction Biomarkers

Xingyu Xia[1,2,*]

[1]State Key Laboratory of Digital Medical Engineering, Jiangsu Key Laboratory for Biomaterials and Devices, School of Biological Science and Medical Engineering, Southeast University, Nanjing, 211189, China
[2]Southeast University-Monash University Joint Graduate School, Suzhou, 215123, China

Abstract. Plasmonic nanomaterials have significantly advanced the detection of trace biomarkers, with Prussian blue (PB) emerging as a prominent candidate in biosensing applications. Traditional Raman reporters often exhibit multiple spectral bands in the fingerprint region, leading to inevitable overlap with endogenous biomolecules. In contrast, PB acts as a highly sensitive, background-free resonance Raman reporter. It presents a single, strong, and sharp band in the cellular Raman silent region, completely resolving its Raman signal from biological species without the need for complex spectral unmixing. In this study, we developed a novel surface-enhanced resonance Raman scattering (SERS) probe with a high signal-to-background ratio (SBR) by assembling PB onto plasmonic gold nanostar (AuNS) cores. Advancing beyond prior PB-based probes, this core-shell design uniquely leverages the tunable anisotropic plasmonic field of the multi-spiked AuNS core to significantly amplify the Raman signal of the PB shell. To maximize the enhancement of the PB SERS signal, we systematically compared AuNS cores with various spike morphologies and identified the optimal core-shell architecture based on maximum SERS intensity and signal reproducibility. The selected AuNS@PB nanoparticles were successfully applied to detect the acute myocardial infarction (AMI) biomarker, Creatine Kinase MB (CK-MB), at extremely low concentrations, fundamentally improving detection sensitivity and accuracy. The optimized SERRS probe achieved an ultra-low limit of detection (LOD) of 10 fg/mL, demonstrating its exceptional potential as a robust platform for the early clinical diagnosis of AMI.

1 Introduction

Cardiovascular diseases (CVDs) remain the primary cause of global mortality, with acute myocardial infarction (AMI) accounting for approximately 20% of these fatalities[1]. Rapid diagnosis is paramount to patient survival, yet initial electrocardiograms (ECG) often lack the sensitivity required for early-stage screening. While Creatine Kinase MB (CK-MB) is a gold-standard biomarker for myocardial necrosis, conventional Enzyme-Linked Immunosorbent Assay (ELISA) kits typically offer a detection limit of (0.05-0.1 ng/mL). This sensitivity is frequently insufficient for capturing the ultra-low concentration fluctuations in the early "golden window" of AMI, potentially delaying critical reperfusion therapy.

Surface-Enhanced Raman Scattering (SERS) has emerged as a revolutionary tool for trace detection due to its ultra-high sensitivity and multiplexing capabilities[2]. However, a persistent challenge in biological SERS sensing is the spectral congestion in the "fingerprint region" (400-1800 cm^{-1}). Endogenous biomolecules in complex serum samples generate significant Raman background, which overlaps with traditional organic reporter signals, necessitating arduous spectral deconvolution and compromising accuracy.

To bypass this interference, Prussian blue (PB) serves as a superior "background-free" resonance Raman reporter. The cyano group (-C≡N) in the PB lattice exhibits a distinct, sharp vibration peak at approximately 2156 cm^{-1}, situated within the biologically "Raman silent region" (1800-2800 cm^{-1}). Since no endogenous biological species contribute to this spectral window, the PB signal can be precisely resolved with an exceptional signal-to-background ratio (SBR) without complex mathematical modeling.

The performance of a SERS probe is fundamentally dictated by the electromagnetic enhancement of the plasmonic substrate. Theoretical models suggest that anisotropic multi-spiked nanostructures, such as gold nanostars (AuNSs), create intense localized electromagnetic fields[3]. This is attributed to the "lightning-rod effect" at the sharp tips and the near-field coupling between adjacent branches, which together generate high-density "hotspots." In this study, we systematically tailored the spike protrusion of AuNS cores to investigate their influence on the SERRS enhancement of the PB shell.

* Corresponding author: xiaxingyu1130@163.com

By integrating the optimized anisotropic AuNS core with a PB shell, we fabricated a highly sensitive AuNS@PB core-shell probe. This optimized architecture demonstrated a remarkable detection limit of 10 fg/mL for CK-MB, representing a several-thousand-fold improvement over mainstream commercial assays. This platform not only provides a robust strategy for the ultra-sensitive early screening of AMI but also offers a universal paradigm for background-free biosensing in complex biological matrices.

2 Materials and methods

2.1 Materials and reagents

$HAuCl_4 \cdot 3H_2O$ (≥49.0% Au basis), $C_6H_5Na_3O_7$ (≥98%), and L-ascorbic acid (AA, ≥99%) were purchased from Sigma-Aldrich. N-hydroxysuccinimide (NHS, 98%), N-(3-dimethylaminopropyl)-N′-ethylcarbodiimide hydrochloride (EDC, 98%), and $FeCl_3 \cdot 6H_2O$ (≥99%) were obtained from Aladdin. Diethylene glycol ($(CH_2OH)_2$, >98%), $AgNO_3$ (99.99%), and concentrated hydrochloric acid (HCl, 37 wt%) were acquired from Macklin. Sodium acetate (CH_3COONa, ≥99.5%), ethylene glycol ($C_4H_{10}O_3$, ≥99.5%), and $K_4Fe(CN)_6 \cdot 3H_2O$ (≥99.5%) were purchased from Greagent. Sodium acrylate ($C_3H_3O_2Na$, 98%), phosphate-buffered saline (PBS, 1×, pH 7.2–7.4), and $K_3Fe(CN)_6$ (≥99%) were obtained from Adamas. CK-MB antigen and CK-MB monoclonal antibody were provided by Beijing Bioss Biotechnology Co., Ltd (Beijing, China).

2.2 Synthesis of AuNS@PB NPs

According to the strategy reported by Tuan Vo-Dinh et al., gold nanostars (AuNS) with different numbers and morphologies of protrusions were synthesized[4]. Using these AuNSs as the core, the surface of the AuNSs was etched with potassium ferricyanide ($K_3Fe(CN)_6$), covering the surface of the AuNSs with CN^- groups, providing sites for the directional growth of the Prussian blue (PB) shell layer. Subsequently, the co-precipitation method was employed, adding both ferrocyanide potassium ($K_4Fe(CN)_6$) and ferric chloride ($FeCl_3$) to the system simultaneously. The two precursors underwent coordination polymerization reactions on the surface of the AuNS@CN nanoparticles, using CN^- as the bridging ligand, combining with Fe^{2+} and Fe^{3+} to form the Prussian blue shell layer. Finally, AuNS@PB core-shell structure nanoparticles were prepared[5].

2.3 Synthesis of Fe_3O_4-COOH NPs

Superparamagnetic carboxy-functionalized Fe_3O_4-COOH nanoparticles were synthesized via a one-pot solvothermal approach. Briefly, iron (III) chloride hexahydrate was dissolved in a mixed solvent of diethylene glycol and ethylene glycol. Subsequently, sodium acetate and sodium acrylate were added as structure-directing and co-precipitation agents, respectively. The resulting homogeneous mixture was transferred to a Teflon-lined autoclave and subjected to a solvothermal reaction at an elevated temperature. Upon completion, the black magnetic products were isolated by magnetic separation. The as-synthesized nanoparticles were washed exhaustively with deionized water and ethanol to remove residual reactants, and finally dried under vacuum to yield the final Fe_3O_4-COOH products[6].

2.4 Preparation of AuNS@PB NPs immune probes

Via electrostatic adsorption, the AuNS@PB nanoparticles were conjugated with anti-CK-MB by mixing the nanoparticle suspension with 10 μg/mL of the antibody[7]. The mixture was vortexed for 5 min and subsequently incubated for 1 h under continuous agitation. To quench unreacted active sites and minimize non-specific adsorption, 100 μL of 1% bovine serum albumin (BSA) was introduced for an additional hour of incubation. The resulting immune-probes were purified through two cycles of centrifugation and washing, and finally resuspended in 1 mL of phosphate-buffered saline (PBS) for subsequent detection.

2.5 Preparation of Fe_3O_4-COOH NPs immune probes

The carboxylic groups on the Fe_3O_4-COOH nanoparticles were activated using an EDC/NHS mixture in phosphate-buffered saline (PBS) under ambient conditions. Following activation, the resulting succinimidyl ester-functionalized nanoparticles were magnetically isolated and washed to remove excess reagents. Anti-CK-MB antibodies were then introduced to the dispersion for covalent conjugation via primary amine groups. To minimize non-specific binding, the residual active sites on the nanoparticle surfaces were passivated with bovine serum albumin (BSA). The final magnetic immune probes were purified through multiple magnetic separation and washing cycles, and subsequently stored in PBS at 4 °C for further applications.

2.6 Preparation of Ab-immobilized MBs and Ab-modified AuNS@PB NPs

The CK-MB antigens were first captured by the antibody-functionalized Fe_3O_4-COOH magnetic probes. Following a thorough washing cycle with PBS to remove unbound proteins, the AuNS@PB SERS tags were introduced to the mixture to form the characteristic "magnetic immunoprobe-antigen-AuNS@PB immunoprobe tag" sandwich architecture. This secondary incubation was performed at room temperature, allowing for the specific recognition between the SERS tags and the captured antigens. The resulting immunocomplexes were then isolated using an external magnetic field, washed to eliminate residual

reagents, and finally redispersed in PBS for subsequent SERS measurements.

3 Results and discussion

3.1 Characterization of AuNS@PB NPs

The fabrication of AuNS@PB core-shell SERRS tags commenced with the seed-mediated growth of anisotropic gold nanostars (AuNSs). By precisely modulating the concentration of silver nitrate ($AgNO_3$) during the synthesis, a series of AuNS cores with varying degrees of spike protrusion were prepared, denoted as S5, S10, S20, and S30 AuNSs, respectively. All AuNS variants maintained a consistent tip-to-tip average diameter of approximately 50 nm.

The subsequent encapsulation of the PB shell involved two integrated steps: the formation of cyano-functionalized AuNSs (AuNS@CN) and the controlled interfacial growth of the PB lattice. Briefly, potassium hexacyanoferrate (III) ($K_3[Fe(CN)]_6$) was employed to coordinate with the AuNS surfaces, where the etching duration was optimized to achieve maximum SERS enhancement without compromising the branched morphology of the nanostars. Following this, the PB shell was synthesized via the simultaneous addition of $K_4[Fe(CN)_6]$ and $FeCl_3$ precursors. To ensure the formation of a well-defined shell rather than independent PB self-nucleation, a controlled precursor addition rate was maintained. The thickness and morphology of the shell were further refined by adjusting the precursor concentrations. Under optimized conditions, the AuNS@PB nanoparticles evolved into a uniform core–shell architecture with a final average diameter of approximately 84 nm.

The structural integrity and elemental distribution of the resulting AuNS@PB NPs were characterized using transmission electron microscopy (TEM) and high-angle annular dark-field scanning transmission electron microscopy (HAADF-STEM). As illustrated in the HAADF-STEM and EDX elemental mapping images (Figure 1), the nanoparticles exhibit a distinct core–shell morphology. The elemental mapping results provide direct evidence of the spatial arrangement: the Au signal (green) is highly localized within the branched central core, while the Fe (cyan) and K (yellow) signals, characteristic of the Prussian blue lattice, are homogeneously distributed across the outer shell. Furthermore, the Ag signal (red) confirms the role of silver in directing the anisotropic growth of the nanostar tips. These results collectively confirm that the multi-spiked AuNS cores are encapsulated by a continuous and uniform PB shell, providing a robust platform for high-performance SERS sensing.

The crystalline structure of the as-prepared AuNS@PB core-shell nanoparticles was confirmed by powder X-ray diffraction (XRD) analysis. As illustrated in Figure 2, the XRD pattern clearly displays the characteristic diffraction peaks of both gold and Prussian blue. Specifically, the peaks corresponding to the gold core match well with the standard face-centered-cubic (fcc) gold structure (JCPDS card no. 04-0784). Meanwhile, the other distinct peaks are assigned to the fcc lattice of Prussian blue (JCPDS card no. 73-0687). The presence of both sets of diffraction peaks, without any obvious impurity signals, confirms the successful formation and high purity of the core–shell heterostructure.

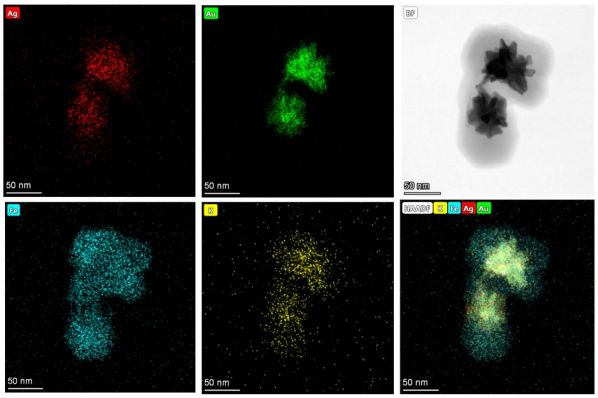

Figure 1. Structural and compositional characterization of the AuNS@PB core–shell nanoparticles. The panels display the bright-field (BF) STEM image (top right) and the corresponding energy-dispersive X-ray (EDX) elemental maps of Ag (red), Au (green), Fe (cyan), and K (yellow), along with the merged HAADF overlay image (bottom right). The mapping results confirm the spatial localization of the branched AuNS core and the uniform PB shell. Scale bars are 50 nm.

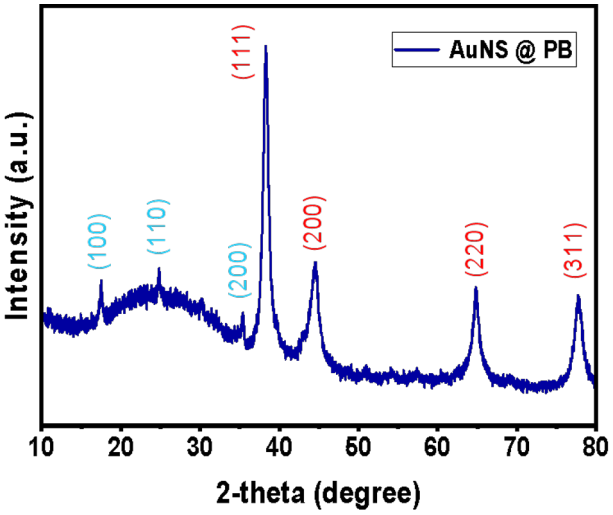

Figure 2. X-ray diffraction (XRD) pattern of the AuNS@PB core-shell nanoparticles. The characteristic diffraction peaks labeled in red correspond to the face-centered-cubic (fcc) structure of the gold core, while the peaks labeled in light blue belong to the fcc lattice of the Prussian blue shell.

3.2 SERS performance of AuNS@PB regulated by the anisotropic spiked core architecture

To investigate the influence of the anisotropic core architecture on the SERS performance, a series of AuNS@PB nanoparticles with varying degrees of spike protrusion were synthesized and evaluated. The morphology of the AuNS cores was precisely modulated by adjusting the concentration of silver nitrate ($AgNO_3$)

from 0.5 mM to 3.0 mM during the seed-mediated growth, yielding samples denoted as S5, S10, S20, and S30 AuNS@PB, respectively.

As illustrated in Figure 3, all prepared samples exhibit a prominent Raman peak at approximately 2156 cm^{-1}, which is assigned to the stretching vibration of the cyano group (-C≡N) in the Prussian blue shell. Compared to pure PB NPs, which display a relatively weak Raman signal, all AuNS@PB nanostructures demonstrate significant signal amplification, confirming the effective electromagnetic enhancement provided by the plasmonic cores. More importantly, the SERS intensity exhibits a clear morphology-dependent trend. As the $AgNO_3$ concentration increases from S5 to S30, the intensity of the 2156 cm^{-1} peak gradually intensifies, reaching its maximum in the S30 AuNS@PB sample. This remarkable enhancement is primarily attributed to the increased degree of spike protrusion on the AuNS cores. The sharper and more abundant branches in the S30 configuration induce a stronger "lightning-rod effect" and generate higher-density localized electromagnetic hotspots, thereby maximizing the SERS signal of the encapsulating PB shell. Consequently, the S30 AuNS@PB nanoparticles were selected as the optimal SERRS tags for all subsequent trace-level biomarker detection assays.

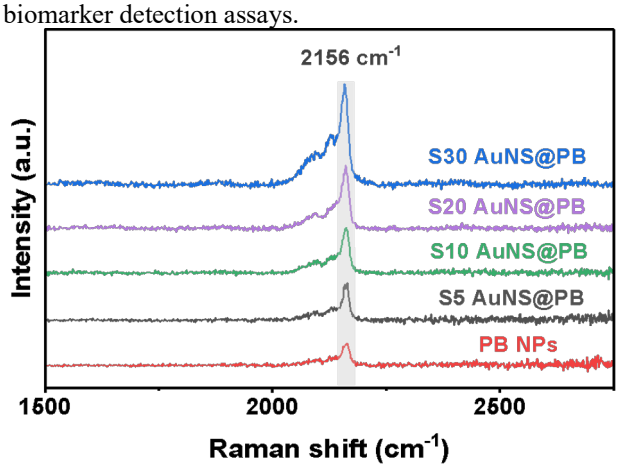

Figure 3. SERS Spectra of AuNS@PB with Different Core Morphologies. SERS spectra of pure PB NPs and varying AuNS@PB core–shell nanoparticles (S5, S10, S20, and S30) synthesized with different concentrations of $AgNO_3$. The shaded area highlights the characteristic Raman peak at 2156 cm^{-1} corresponding to the cyano group (-C≡N) stretching vibration in the Raman-silent region.

3.3 Characterization of Fe_3O_4-COOH

The carboxyl-functionalized magnetic nanoparticles (Fe_3O_4-COOH) were successfully synthesized via a facile one-pot solvothermal method, serving as the robust capture substrates for the SERRS immunoassay. The morphological features of the as-prepared magnetic beads were first investigated using scanning electron microscopy (SEM). As depicted in Figure 4, the Fe_3O_4-COOH nanoparticles exhibit a well-defined spherical morphology with an average diameter of approximately 200 nm. Notably, the nanoparticles display a distinctively rough, raspberry-like surface texture. This structural characteristic is highly advantageous, as it significantly increases the specific surface area of the beads, thereby providing abundant carboxyl active sites for the subsequent high-density covalent conjugation of capture antibodies.

Furthermore, the macroscopic magnetic responsiveness of the solid Fe_3O_4-COOH powder was evaluated. As illustrated in the optical photographs (Figure 4 bottom), the as-synthesized nanoparticles present as a fine brown powder at the bottom of the glass vial. Upon the application of an external magnetic field to the sidewall, the dry magnetic powder rapidly migrates and firmly adheres to the inner wall adjacent to the magnet. This strong magnetic attraction confirms the excellent magnetic properties of the synthesized nanoparticles, providing a solid foundation for the rapid, centrifugation-free isolation of immunocomplexes during the subsequent liquid-phase immunoassay.

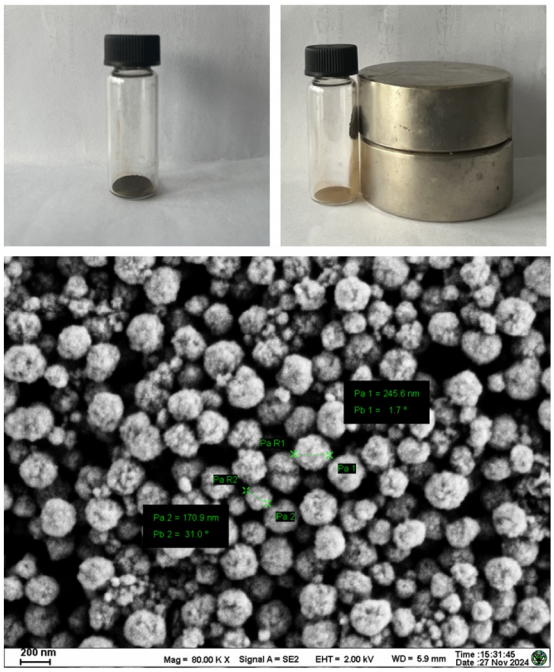

Figure 4. Morphology and magnetic property characterization of the synthesized carboxyl-functionalized magnetic nanoparticles (Fe_3O_4-COOH). The top panels display photographs of the magnetic nanoparticles in a glass vial before (left) and after (right) the application of an external magnetic field, demonstrating their excellent magnetic responsiveness and facile magnetic separation capability. The bottom panel shows the scanning electron microscopy (SEM) image of the Fe_3O_4-COOH nanoparticles, revealing their well-defined spherical morphology and rough surface structure.

3.4 Quantitative detection of CK-MB antigen

Under the optimized experimental conditions, the analytical performance of the proposed sandwich SERRS immunoassay for CK-MB detection was systematically evaluated. A series of CK-MB standard solutions with varying concentrations were introduced into the detection system. As expected, the SERS intensity of the characteristic cyano band at 2156 cm^{-1} increased gradually with the increment of CK-MB

concentration, owing to the capture of more AuNS@PB tags by the magnetic immunoprobes.

To precisely quantify the biomarker, a calibration curve was plotted based on the relationship between the SERS intensity and the CK-MB concentration. As depicted in Figure 5, a distinct linear correlation is established between the SERS intensity and the logarithm of the CK-MB concentration (lg C) across a broad dynamic range from 10 fg/mL to 10 ng/mL. The corresponding linear regression equation is derived as y = 186.48x + 50.65, with a highly reliable correlation coefficient (R^2 = 0.991), where y represents the SERS intensity and x represents the logarithmic concentration of CK-MB (fg/mL). Furthermore, the remarkably small error bars derived from parallel measurements demonstrate the excellent reproducibility and stability of the background-free SERS platform. Based on this robust linear relationship, the limit of detection (LOD) was calculated to be down to 10 fg/mL. Such extraordinary sensitivity is several orders of magnitude superior to that of conventional ELISA kits, successfully meeting the rigorous requirements for the ultra-trace analysis of CK-MB in the early clinical diagnosis of acute myocardial infarction (AMI).

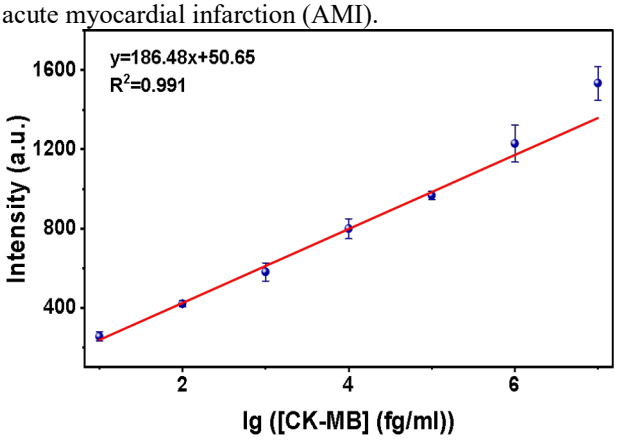

Figure 5. Linear calibration curve for the SERS-based quantitative detection of CK-MB. The plot demonstrates the linear relationship between the SERS intensity at 2156 cm^{-1} and the logarithm of the CK-MB concentration (lg C) spanning from 10 fg/mL to10 ng/mL. The linear regression equation is y = 186.48x + 50.65 with a correlation coefficient (R^2) of 0.991. Error bars represent the standard deviations calculated from three independent replicate measurements.

4 Conclusions

In summary, we successfully developed a novel surface-enhanced resonance Raman scattering (SERS) probe by assembling a Prussian blue (PB) shell onto anisotropic gold nanostar (AuNS) cores for the highly sensitive detection of the acute myocardial infarction (AMI) biomarker CK-MB. This AuNS@PB architecture utilizes PB as a background-free resonance Raman reporter, producing a distinct -C≡N peak at approximately 2156 cm^{-1} within the cellular Raman silent region. This unique property ensures that the signal is completely resolved from endogenous biological interference without requiring complex spectral deconvolution. By systematically tailoring the spike protrusion of the AuNS cores, we determined that the highly branched S30 configuration generates the highest-density localized electromagnetic hotspots via the "lightning-rod effect", thereby maximizing the signal amplification of the encapsulating PB shell. Utilizing this optimized AuNS@PB probe, the quantitative detection of CK-MB exhibited a broad linear dynamic range from 10 fg/mL to 10 ng/mL and achieved an extraordinary limit of detection (LOD) of 10 fg/mL. This remarkable sensitivity fundamentally improves upon conventional ELISA kits, successfully meeting the rigorous requirements for ultra-trace analysis in the early clinical diagnosis of AMI. Ultimately, this platform not only provides a robust strategy for ultra-sensitive early AMI screening but also serves as a universal paradigm for background-free biosensing in complex biological matrices.

References

1. Roth, G.A., et al., *Global Burden of Cardiovascular Diseases and Risk Factors, 1990–2019.* JACC, 2020. **76**(25): p. 2982-3021.
2. Langer, J., et al., *Present and Future of Surface-Enhanced Raman Scattering.* ACS Nano, 2020. **14**(1): p. 28-117.
3. Chung, T. and S.-H. Lee, *Quantitative Study of Plasmonic Gold Nanostar Geometry Toward Optimal SERS Detection.* Plasmonics, 2022. **17**(5): p. 2113-2121.
4. Yuan, H., et al., *Gold nanostars: surfactant-free synthesis, 3D modelling, and two-photon photoluminescence imaging.* Nanotechnology, 2012. **23**(7): p. 075102.
5. Liu, S., et al., *Engineered Core–Shell Multifunctional Nano-Tracer in Raman-Silent Region with Highly Retained Affinity to Enhance Lateral Flow Immunoassays.* Small, 2022. **18**(45): p. 2204859.
6. Xuan, S., et al., *Tuning the Grain Size and Particle Size of Superparamagnetic Fe3O4 Microparticles.* Chemistry of Materials, 2009. **21**(21): p. 5079-5087.
7. Zhang, X., et al., *A bifunctional core–shell gold@Prussian blue nanozyme enabling dual-readout microfluidic immunoassay of food allergic protein.* Food Chemistry, 2024. **434**: p. 137455.